Journal of Colloid and Interface Science 442 (2015) 133–139

Contents lists available at ScienceDirect

Journal of Colloid and Interface Science

www.elsevier.com/locate/jcis

Effect of water absorption on pollen adhesion

Haisheng Lin [a], Leonardo Lizarraga [b], Lawrence A. Bottomley [b,*], J. Carson Meredith [a,*]

[a] School of Chemical & Biomolecular Engineering, Georgia Institute of Technology, 311 Ferst Drive NW, Atlanta, GA 30332-0100, United States
[b] School of Chemistry & Biochemistry, Georgia Institute of Technology, 901 Atlantic Drive, Atlanta, GA 30332-0400, United States

ARTICLE INFO

Article history:
Received 19 September 2014
Accepted 27 November 2014
Available online 4 December 2014

Keywords:
Sunflower pollen
Pollenkitt
Atomic force microscopy
Force spectroscopy
Adhesion
Humidity
Microcantilever sensor
Capillary forces

ABSTRACT

Pollens possess a thin liquid coating, pollenkitt, which plays a major role in adhesion by forming capillary menisci at interfaces. Unfortunately, the influence of humidity on pollenkitt properties and capillary adhesion is unknown. Because humidity varies widely in the environment, the answers have important implications for better understanding plant reproduction, allergy and asthma, and pollen as atmospheric condensation nuclei. Here, pollenkitt-mediated adhesion of sunflower pollen to hydrophilic and hydrophobic surfaces was measured as a function of humidity. The results quantify for the first time the significant water absorption of pollenkitt and the resulting complex dependence of adhesion on humidity. On hydrophilic Si, adhesion increased with increasing RH for pollens with or without pollenkitt, up to 200 nN at 70% RH. In contrast, on hydrophobic PS, adhesion of pollenkitt-free pollen is independent of RH. Surprisingly, when pollenkitt was present adhesion forces on hydrophobic PS first increased with RH up to a maximum value at 35% RH (~160 nN), and then decreased with further increases in RH. Independent measurement of pollenkitt properties is used with models of capillary adhesion to show that humidity-dependent changes in pollenkitt wetting and viscosity are responsible for this complex adhesion behavior.

1. Introduction

Pollen particles, carrying the male gamete of plants, possess a range of unique ornamentations with various morphologies and feature sizes. They can effectively disperse in air or entangle with hairs on animals allowing for their distribution over large areas. Understanding the adhesion mechanisms of pollen particles is of scientific interest due to their role in plant reproduction [1], the health of pollinators [2,3], human environmental health [4], and ice and water formation in the atmosphere [5,6]. For example, consider that the maintenance of healthy bee communities, which has a complex interdependent relationship with pollination ecology, is of current worldwide concern [2,3]. In addition, proteins carried on pollens contribute to asthma and allergies in humans and the pollen grain's adhesive capabilities are significant factors in pollen environmental distribution [7]. Finally, pollen grains are known to be carried into the atmosphere where they can absorb organic pollutants, age under UV exposure, and act as nucleation sites for water condensation or ice formation [8]. Therefore, their surface properties and sensitivity to humidity are of interest due to their potential role in climate and weather. Due to their unique geometrical features that enable fine-tuning of adhesion, pollens have been recently explored as a bio-organic template for the synthesis of biomimetic functional materials in a variety of applications [9–12], including adhesives, composites, paints and pigments, drug delivery, and porous media for sensors, adsorbents, catalyst supports and filtration [13,14]. Despite the wide range of fields influenced by pollen properties, there still is a lack of quantitative understanding of pollen surface properties and how these affect adhesion and release characteristics. In particular, one of the compelling unresolved questions is the role of the liquid pollenkitt coating in carrying water and mediating the sensitivity of pollen adhesion to the effects of humidity.

The pollen exine shell is composed predominantly of sporopollenin [15–18], a crosslinked polymer which is one of the most chemically-stable naturally-occurring materials, and has good thermal and mechanical stability [19,20]. Pollen grains are additionally coated with a liquid that resides on or within cavities in the exine wall [21]. This coating material (named pollenkitt by Knoll [21]) is especially prevalent in pollen from *entomophilous* plants, and is a mixture composed of saturated and unsaturated lipids, and lesser amounts of carotenoids, flavonoids, proteins and carbohydrates, and is of great importance in pollination ecology [4,15]. It is generally thought to occur as a water-in-oil

* Corresponding authors.
E-mail addresses: lawrence.bottomley@chemistry.gatech.edu (L.A. Bottomley), carson.meredith@chbe.gatech.edu (J. Carson Meredith).

http://dx.doi.org/10.1016/j.jcis.2014.11.065
0021-9797/

emulsion in nature, i.e., there exists an aqueous phase of dispersed water droplets that may also contain polar organics. The dispersal of entomophilous pollens is thought to be facilitated by pollenkitt's ability to keep pollen grains together during transport and to promote adhesion to animals. It is known that these pollinators eat pollenkitt and that pollenkitt is an important source of nutrients. Pollenkitt is also thought to play a role in adhesion of pollen to the stigma, an important prerequisite for cell recognition and pollen germination [1].

In previous work, we described how pollen adhesion is quantitatively dependent on both a dry mechanism controlled by van der Waals forces and the size of ornamentations, and a 'wet' mechanism controlled by the capillary forces of pollenkitt liquid bridges between pollen and a substrate surface [22]. However, despite the wide variation of humidity in nature, surprisingly little is known about the water content of pollenkitt as a function of humidity, or the effect that water uptake has on capillary-driven adhesion mediated by pollenkitt. In the present work, the adhesion forces between sunflower pollen grains with and without pollenkitt were studied on both hydrophilic silica-coated silicon (Si) and hydrophobic polystyrene (PS) surfaces were studied as a function of relative humidity (RH) by using atomic force microscopy (AFM). We describe below our finding that pollenkitt indeed absorbs a significant amount of water and that this water uptake has a marked effect on the adhesion of pollen to hydrophilic and hydrophobic surfaces. The adhesion forces are modeled and the wetting properties and viscosity of pollenkitt are also determined independently, in order to elucidate their role in RH-dependent adhesion of pollenkitt.

2. Materials and methods

2.1. Pollen and substrate preparation

Piranha-etched Si wafers were used as hydrophilic reference surfaces, since they are coated with a thin layer of silicon oxide. Hydrophobic PS (M_w = 230,000, Sigma–Aldrich) surfaces were prepared by knife-edge coating 10% m/m in PS/toluene solutions on Piranha-etched silicon substrates [23], followed by drying at room temperature for 24 h and annealing at 60 °C under vacuum for 2 h. Film thickness, measured with interferometry, was approximately 1–2 μm, which far exceeds the range of van der Waals interactions (~20 nm) of the underlying silicon substrate. The mean (R_a) and root-mean-square (rms) roughnesses of Si and PS surfaces were 0.2 ± 0.1 and 0.3 ± 0.1 nm, 2.2 ± 0.2 and 2.7 ± 0.2 nm, respectively, obtained from topography scans of three random 10 μm × 10 μm areas using AFM (Veeco Dimension 3100).

Sunflower, a widespread flowering plant, produces pollen with uniform size and morphology consisting of well-organized nanoscale-spiny features. Sunflower pollen is entomophilous and carries a liquid pollenkitt coating whose composition has been characterized previously [24], and represents an ideal model for this study [8,25]. Non-defatted sunflower (*Helianthus annuus*) pollen, containing pollenkitt (PK+, Greer Laboratories, Lenoir, NC) was stored at 0 °C. To provide a pollenkitt-free control (PK−), we washed PK+ with chloroform:methanol (3:1) [26] solution for 24 h (a solvent for external pollenkitt, but non-solvent for sporopollenin) prior to depositing on filter paper (P5, Fisher Scientific, Pittsburgh, PA) and drying in air.

2.2. Force measurements

Adhesion was measured by using a NanoScope IIIA Multimode AFM (Veeco Metrology, Santa Barbara, CA) with tipless rectangular cantilevers (Applied NanoStructures, Inc., Santa Clara, CA, nominal spring constants of 1.2–6.4 N/m). Single pollen grains were glued to tipless cantilevers with epoxy resin using a procedure described elsewhere [27]. The spring constants for cantilevers with attached pollen, determined by methods described elsewhere [28,29], were 2.1–2.3 N/m for PK+ and 1.8–1.9 N/m for PK−. A series of ten force-distance curves were measured for each combination of pollen tip (PK+ or PK−)-substrate (PS or Si), on three separate substrates within three randomly chosen 10 μm × 10 μm areas, under a nitrogen/water atmosphere (20 °C) with controlled relative humidity. Each experiment commenced by cycling the scanner in z direction for ~1 h to allow the scanner to reach thermal equilibrium. Adhesion measurements were performed by extending the scanner over a ~500 nm distance at 10 nm/s until contact with the surface, at which point scanner extension was continued until a loading force of 200 nN was reached, followed by scanner retraction at 10 nm/s. Force versus distance curves were generated by multiplying the measured downward deflection of the cantilever times the spring constant of the cantilever. The force-distance data indicated that only one spine makes contact with the substrate [22].

2.3. Mass uptake measurements in humid air

Thermal resonance data was acquired simultaneously with force data by taking raw (prior to analog filtering) vertical deflection, horizontal deflection and summed signals directly from the AFM and routing them into a PCI-6120 data acquisition card through a BNC-2110 interface (National Instruments, Austin, TX). The pollen-loaded cantilever resonated at its natural thermal resonance frequency; no external oscillation was applied to the cantilever holder. To correlate these signals with scanner movement in the z dimension, the z scanner voltage was taken from the signal access module and sent to the data acquisition card. Data acquisition software written in LabVIEW (National Instruments, Austin, TX) converted the deflection data into the frequency domain (i.e., power spectral density) using the discrete Fourier transform with a Blackman–Harris window. Cantilever resonance data was acquired with a sampling rate of 800 kHz with a 50 Hz resolution along the frequency axis of the power spectral density. To improve the signal-to-noise ratio, an average of fifteen FFTs was taken. Frequency shifts, Δf, are measured at all RH values relative to the lowest RH of 17%. The relationship between mass increase (Δm) and frequency shift, Δf, as water is taken up by the pollen sample (by condensation, adsorption or absorption) can be determined from a single-degree-of-freedom (SDOF) approximation, as described in detail in supplementary material (see Fig. S1 and corresponding discussion in supplementary material). In this manner, all mass changes, Δm, are relative to the lowest RH of 17%.

2.4. Control and variation of relative humidity

The AFM was enclosed in a plastic chamber into which a stream of N_2 gas with controlled RH is introduced, allowing investigation of the effect of humidity on the AFM force measurements. Relative humidities between 15% and 70% were achieved by adjusting the flow rate ratio of as-received dry N_2 gas (UHP300, Airgas USA, LLC.) and N_2 gas bubbled through water.

2.5. Scanning electron microscopy (SEM)

The pollen AFM probes were characterized by scanning electron microscopy (Zeiss Ultra60 FE-SEM) after all force measurements were finished, at an accelerating potential of 10.0 kV. Probe tips were sputtered with gold and then mounted on metal stubs using carbon tapes.

2.6. Contact angle measurements

Contact angles of pollenkitt–water mixtures were measured at 20 °C on the Si and PS substrates using a video contact angle system (AST products 2500XE, Billerica, MA). Nine 1 μL drops of each liquid of the mixture of pollenkitt and water were dispensed onto different regions of the PS surfaces. Both the right and left angles between the sample surface and the tangent line to each droplet were measured for each droplet.

2.7. Viscosity measurement

The viscosities of water-rich pollenkitt–water mixtures (50–100% water) were measured at 20 °C (30% RH) by using an Ostwald viscometer with DI water as a calibration liquid. The viscosities of water-lean pollenkitt–water mixtures (0–10% water) were much higher than the water-rich mixtures and were measured by using an MCR 300 controlled stress rheometer (Anton Paar) with a standard couette geometry (CC17: inner cup diameter = 18.08 mm and bob diameter = 16.66 mm) in small deformation oscillatory mode.

3. Results and discussion

The cantilevers with PK− and PK+ pollen grains attached are shown in Fig. 1. The SEM images, taken after force measurements were completed, show no damage to pollen grains occurred during measurement of adhesive force. Fig. 1(a) and (c) also show that pollenkitt on PK+ can be seen to fill cavities and pores in the exine (Fig. 1a) while the SEM of PK− shows that pollenkitt has been removed as evidenced by open cavities and pores.

The fundamental resonance frequencies, f, of the pollen-loaded AFM cantilevers for each RH and substrate are plotted in Fig. S2 (supplementary material). With increasing RH, f decreases for both PK− and PK+ samples, indicating added mass. For the tipless cantilever with no pollen attached (both bare and coated with a small amount of epoxy resin), f decreased by ~10 Hz from the lowest (17%) to the highest (70%) humidity. This is in agreement with the previously-reported mass uptake of the cantilever upon water condensation [30]. Although the viscosity and density of N_2/water gas decreases with increasing humidity, the change in density and viscosity are small over the range in humidity studied herein and produce a negligible shift in resonance frequency [31]. For the sunflower pollen tips, f decreased by ~450 Hz (PK−) and 700 Hz (PK+) from the lowest (17%) to the highest humidity (70%). The changes of f indicate a larger amount of water absorption by the sunflower pollen when pollenkitt is present. Independent tests confirmed that no significant change in the frequency with humidity was observed due to the presence of the small amount of epoxy used to glue the pollen grains.

By using the SDOF model, we first measured the mass of single cleaned (PK−) and non-defatted sunflower pollen (PK+) grains to be 102 ± 8 ng and 115 ± 7 ng, respectively. The amount of pollenkitt on each PK+ grain is 13 ± 8 ng and represents ~10% of the total mass of a single PK+ grain, consistent with previous values [22,32]. The thickness of pollenkitt on the PK+ shell estimated by SEM images was 10–20 nm. Shown in Fig. 2 is the mass of water absorbed at each RH, relative to the lowest RH value (17%), calculated from frequency shifts. Fig. 2 also shows the water content as a percentage of the mass of "dry" pollenkitt (at 17% RH) carried on a single pollen. The mass of PK− sunflower pollen increased by 0.6 ng at the highest humidity of 70%, or 0.6% of the PK− pollen dry mass.

The water taken up on PK− may be adsorbed onto the external surface area, absorbed into the sporopollenin, or condensed in the pores. Estimates of the water capacity of each of these mechanisms (given in supplementary material) show that 0.6 ng is a reasonable value for water uptake. Calculations based on measured surface areas of ragweed pollens show that the external surface of one pollen grain could adsorb ~0.03–0.15 ng water as a monolayer, accounting for up to 25% of the observed 0.6 ng. By using the solubility of water in poly(ethylene terephthalate) as a guide, it can be estimated that approximately 0.4 ng could be absorbed (dissolved) in a 102 ng mass equal to that of the average sunflower pollen mass [33]. Finally, a rough estimate of the water mass that could condense in the apertures (pores) on the PK− surface yields 3×10^{-6} ng condensed per 100 nm aperture. Given that a single pollen contains on the order of a few hundred pores, clearly the condensed water capacity is too small to account for a significant part of the 0.6 ng water uptake. We conclude that adsorption and

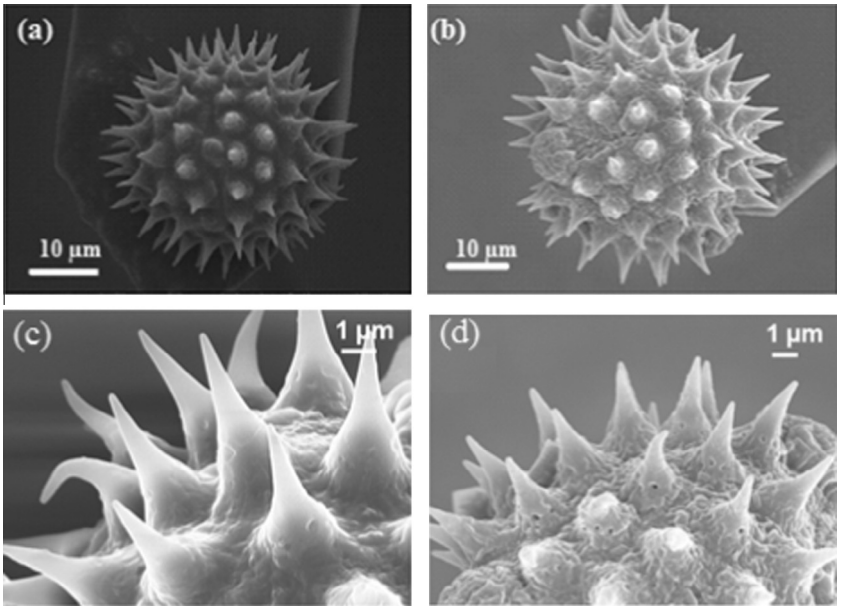

Fig. 1. Low and high magnification SEM micrographs of AFM probes of PK+ ((a) and (c)) and PK− ((b) and (d)) sunflower pollen after all AFM force measurements were completed.

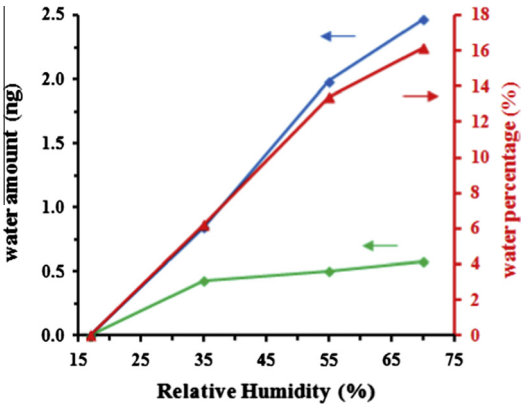

Fig. 2. Measured water uptake onto pollen as a function of RH (blue: PK+; green: PK−). The red line shows water uptake as % of dry pollenkitt mass for PK+ sunflower pollen. (For interpretation of the references to color in this figure legend, the reader is referred to the web version of this article.)

absorption likely account for most of the water uptake on PK− pollen.

The amount of water taken up by PK+ is much larger than by PK−, approximately 4× higher at 70% RH (Fig. 2). This result suggests that the additional water uptake on PK+ is due to absorption into the liquid pollenkitt coating itself. This amount is feasible because pollenkitt possesses both polar organic compounds as well as an aqueous droplet phase that have significant capacity for water uptake. As shown in Fig. S3 (supplementary material), at high RH the absorbed water expands the volume of the droplets distributed as a minor phase in the pollenkitt emulsion. Fig. 2 indicates that the amount of water absorbed at the highest RH is about 16% of the "dry" pollenkitt mass. These are the first reported values of the absorption of water as a function of RH% for pollenkitt on pollen. It has been suggested in the literature that one important function of pollenkitt is preventing water loss during pollen transport and the water absorption within pollenkitt measured here supports this idea [32]. Our adhesion results below also indicate that the water-absorbing capacity of pollenkitt also plays in important role in pollen adhesion.

The measured adhesion pull-off forces versus relative humidity (RH) for sunflower pollens (PK+ and PK−) interacting with PS and Si substrates are shown in Fig. 3. Fig. 4 shows typical force-distance curves of PK− and PK+ sunflower pollen on Si as a function of RH (plots for PS are given in supplementary data Fig. S4 and differ in magnitude only). From Fig. 3 one observes that on PS no

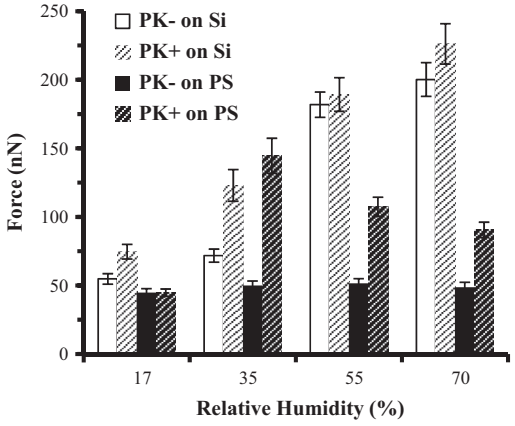

Fig. 3. Pull-off adhesion forces of PK− and PK+ sunflower pollen on Si and PS substrates versus RH. Error bars are 95% confidence intervals.

dependence on RH is observed over the entire RH range of 17–70%, explained by the hydrophobic character of PS. Although stable condensed water films can form in a nanoscale gap between approaching surfaces at RH > 40% [34], an adhesive capillary bridge will not form due to nonwetting behavior of water on PS (contact angle: 101.1 ± 3.0°). On Si at low RH (RH < 35%), stable water films capable of forming capillary bridges are not expected to condense [34] and the adhesion is mainly governed by van der Waals forces [22]. However, at RH > 35%, the adhesion force on Si significantly increases, suggesting that water condenses between the pollen tip and the hydrophilic Si surface. Because some degree of wettability is required for formation of an attractive capillary neck, the results indicate that water wets sporopollenin, although the contact angle is unknown. The water-mediated capillary adhesion force, F_c, of PK− pollen can be modeled by considering a meniscus in nanoscale contact between a sphere (pollen spine tip) and a flat plane [34]

$$Fc = \pi\gamma R\cos\theta\frac{(1+\cos\beta)^2}{\cos\beta} \quad (1)$$

where γ is the water surface tension (0.0728 N m^{-1}), R is the tip radius (120 nm), β is the filling angle between the normal and the meniscus contact line on the tip, and θ is the contact angle of water on the substrate. The angle β increases with the volume of condensed water in the capillary bridge, which increases with RH according to the Kelvin equation, leading to an increase of adhesion force with RH. Fig. S5 in supplementary materials shows the relationship between F_c and β as calculated with Eq. (1).

A noticeable feature in Fig. 4a and b is that at all RH values, upon retraction, the two solids separate suddenly at the maximum adhesion force between PK− and the substrate. Sudden pull-off transitions are clearly expected in the case of dry solid–solid short-ranged adhesion [22]. However, liquid capillary bridges that form at high RH sometimes show more gradual pull-off during which the capillary neck is thinning while still attached to both surfaces. Our observation of a sudden pull-off (Fig. 4b) is however consistent with previous reports of pure water capillary forces. The high surface tension and low viscosity of water drive a relatively rapid thinning and rupture of the bridge [35].

The PK+ pollens, containing native pollenkitt, behaved quite differently from PK−. As the results show in Fig. 4c and d (as well as Figs. S4c and S4d for PS, supplementary material), as the PK+ AFM tip approaches Si, it experiences a jump to contact attraction attributed to the attractive capillary force arising from the wetting of pollenkitt liquid, also observed in our previous study performed at 30% RH [22]. At the lowest humidity of 17% RH, shown in Fig. 4c, during retraction the attractive force increased to a maximum value at a distance of ~140 nm for Si. After that, a long-range, gradual adhesive force was observed, which always decayed with increasing distance. The shape of this long-range adhesive force upon pull off is consistent with the formation, thinning, and rupture off a viscous capillary neck [35,36]. One requirement for capillary bridge formation due to pollenkitt (in PK+) is the wetting of pollenkitt on both substrate and pollen. The contact angles of extracted pollenkitt on Si and PS were measured previously to be 16° and 43° at ~30% RH [22], and pollenkitt is known to fully wet the pollen shell. The magnitude of these values and relative preference for wetting Si versus PS was also confirmed by measuring contact angles of prepared pollenkitt–water mixtures, as discussed below with Fig. 5.

In order to test the idea that capillary meniscus forces are responsible for the long-range pull-off observed in Fig. 4c for Si (as well as Fig. S4c for PS), we used a capillary force model to fit the long-range adhesive forces. Upon retraction, the adhesive force of a liquid bridge can have both a capillary contribution (due to the

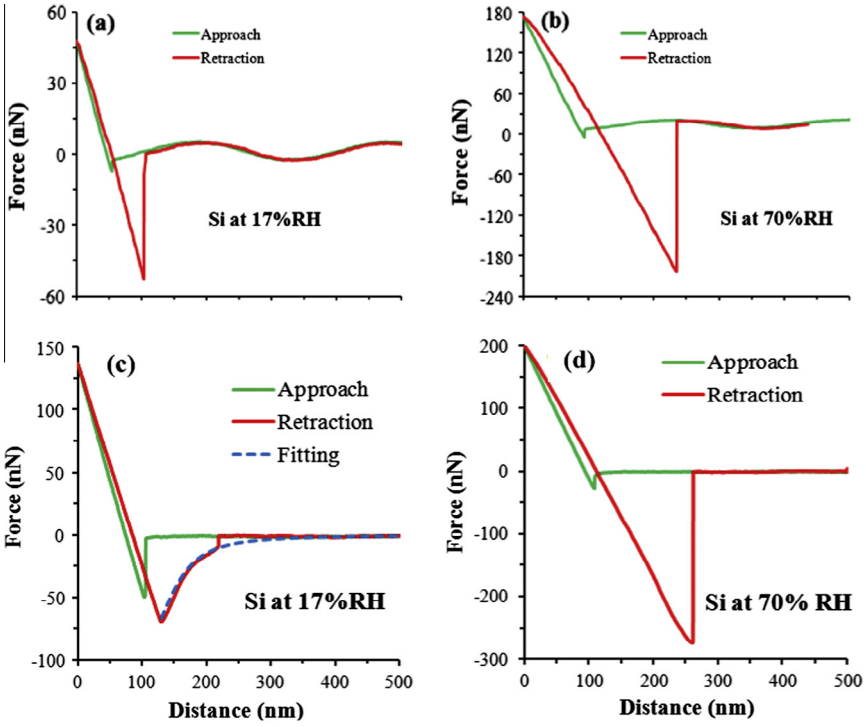

Fig. 4. Typical AFM force-distance curves of PK– (a and b) and PK+ (c and d) on Si under relative humidities of 17% and 70%. The blue dashed line in (c) represents the theoretical capillary force as a function of distance calculated with $\gamma = 0.045$ Nm^{-1}, $R = 120$ nm, and $c = 0.998$, $V = 11.62 \times 10^5$ nm^3, according to Eq. (2).

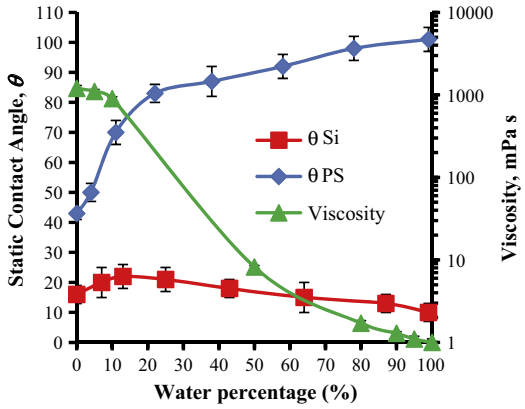

Fig. 5. Dynamic viscosity and static contact angles of pollenkitt–water mixtures on Si (red line) and PS (blue line) surfaces versus water percentage in the mixture. (For interpretation of the references to color in this figure legend, the reader is referred to the web version of this article.)

surface tension and Laplace pressure across the curved meniscus), as well as an adhesive force due to viscous resistance to capillary thinning. For a liquid bridge with constant volume, V, the equilibrium capillary meniscus force is [37]

$$Fc = 4\pi\gamma cR\left(1 - \frac{D}{\sqrt{\frac{V}{\pi R} + D^2}}\right) \quad (2)$$

$$c = \frac{\cos(\theta_1 + \beta) + \cos\theta_2}{2} \quad (3)$$

where γ is liquid surface tension (0.045 N m^{-1} for pollenkitt at 30% RH [22]), R is sphere radius (120 nm), β is filling angle, θ_1 and θ_2 are the contact angles of liquid to sphere and to the plane, respectively, and D is the distance between the sphere and the planar surface. V was assumed to be constant, since the exposure of pollenkitt to humid N_2 (17% RH) reaches a steady-state prior to performing the AFM experiments, and observations show that drops of PK do not evaporate in air. According to our previous measurement and calculation, the filling angle β for pollenkitt between a non-defatted sunflower pollen and various surfaces was ~20° [22]. Here we can obtain c from Eq. (3) as 0.997 and 0.768 for Si and PS surface, respectively, at contact ($D = 0$). In Fig. 4c (and Fig. S4c, supplementary data), using V and c as fitting parameters, the blue fitting lines showed that the calculated curves fit very well with the experimental retraction results. The values of c obtained by experimental force curves are roughly within 10% error of the values calculated by Eq. (3) (Table S1). The curves could also be fitted with $V = 11.63 \pm 0.24 \times 10^5$ nm^3 and $1.03 \pm 0.04 \times 10^5$ nm^3 for Si and PS surfaces, respectively. From the fitting, the volume of a pollenkitt bridge between PK+ and Si is ~10 times higher than with PS, which is consistent with better pollenkitt wetting on a Si surface (discussed below with Fig. 5). These trends in volume also support the observation of a much longer range of separation distance on the Si surface (from ~140 nm to ~300 nm, Fig. 4c) compared to the PS surface (from ~180 nm to ~250 nm, Fig. S4c).

Above, we neglected the viscous contribution to capillary forces, because the viscous force is estimated to be several orders of magnitude smaller than the observed forces. The hydrodynamic force (F_h) of the pollenkitt liquid bridge during retraction is estimated a no-slip flow between a sphere and a flat surface [35,38,39]:

$$Fh = 6\pi\eta R^2\left[1 - \frac{D}{\sqrt{\frac{V}{\pi R} + D^2}}\right]^2 \frac{1}{D}\frac{dD}{dt} \quad (4)$$

where η is dynamic viscosity, R is tip radius, D is separation distance, and dD/dt is retraction velocity. F_h is attractive upon retraction, but its magnitude is only 0.02 nN at contact, which is much smaller than observed force magnitudes. (We used a value of $\eta = 1.2$ Pa s for pollenkitt at 17% RH determined by rheology as

described below with Fig. 5.) At these conditions the viscous forces do not make significant contributions to adhesion.

In contrast to the PK+ force curve under low humidity (RH < 35%, Fig. 4c), there is an absence of long-range adhesion during pull off at RH > 35%. As shown in Fig. 4d for Si substrates (and Fig. S4d for PS substrates), at RH 70% during approach, the cantilever tip jumped toward the substrate at a distance of ~100 nm (~75 nm for PS) with an attractive force magnitude of ~25 (~10 nN for PS), respectively. When retracting from the substrate at 70% RH, the adhesive pull-off force increased up to ~225 nN (on Si) and ~92 nN (on PS), at which point the tip suddenly jumped to zero force, indicating a sudden rupture of the capillary liquid bridge. In contrast to the low RH (17%) case, there is no long-range decay force associated with a capillary meniscus thinning for the high RH (70%) case.

Eq. (1) suggests that the larger snap-in and adhesive pull-off forces observed for the hydrophilic Si surface (compared to PS) are driven by the better wetting (lower contact angle θ) of pollenkitt on Si than on PS. We also expect that the difference in force curve behaviors for PK+ (pollenkitt-containing pollens) at low and high RH is caused by the change in properties of the pollenkitt as it absorbs water, as well as adsorption of water films on the Si surface that likely occurs. The properties of pollenkitt relevant to capillary forces are surface tension, contact angle on the tip and substrate, and viscosity, each of which should change due to the absorption of water in pollenkitt. As compared to pollenkitt with a surface tension of 0.045 N m^{-1} and a viscosity of ~1.2 Pa s, water has a higher surface tension of 0.0728 N m^{-1} and a significantly lower viscosity of 1.0 mPa s. To explore this idea, we prepared solutions of extracted pollenkitt with water and measured viscosities as well as the contact angles on Si and PS surfaces. As shown in Fig. 5, the dynamic viscosity of the mixture of PK and water decreases with increasing water fraction. The contact angle on PS increases rapidly with increasing water fraction, and the higher contact angle decreases the capillary attractive force (Eqs. (1) or (2) show this) [34]. The results in Fig. 5 also indicate that pollenkitt consistently wets the Si surface with a smaller contact angle than the PS surface. This preferential wetting on Si versus PS becomes more pronounced as the water content increases, and eventually the contact angle on PS becomes nonwetting (>90°) at high water content. This observation is consistent with the observed adhesion force magnitudes on Si compared to PS, which indicate significantly higher volumes of liquid in the bridges on Si and better wetting (as discussed above with Fig. 4 and Fig. S4). The observed ability to wet both a hydrophilic and hydrophobic surface, with preference toward the hydrophilic substrate, is consistent with the significant water capacity of pollenkitt, the polar nature of the organic substances in pollenkitt [4,15], and to the fact that some of the water is actually carried in a droplet phase.

We can now better rationalize the high RH results of Fig. 4 and Fig. S4 based on the viscosity of pollenkitt–water mixtures from Fig. 5. A pollenkitt liquid bridge of lower viscosity (at high RH) will have faster thinning of the capillary meniscus and breakage at smaller distances [35–37], relative to "drier" pollenkitt with higher viscosity. In addition to the viscosity effect, we also should consider that at 70% RH, the thickness of the water layer adsorbed on a Si surface normally is ~4–7 nm [40]. This stable layer of condensed water likely prevents immediate and direct wetting of pollenkitt (from the pollen spine) onto the solid Si substrate. The contact is rather between liquid on the pollen spine (pollenkitt with 16% absorbed water) and the thin layer of water on the Si substrate. There are two possibilities. First, the thin water film could mix completely with the pollenkitt, increasing its water content beyond 16%. Second, if the water film and pollenkitt do not have time to mix during tip approach and retraction (~1 min), then a concentration gradient will exist in the capillary bridge, going from pure water at the Si surface to pollenkitt toward the pollen. In either case, we expect the effect of the pure water film on the Si substrate is to lower the viscosity and raise surface tension of the pollenkitt–water mixture. Thus, just as we observed, a faster rupture at shorter distances would be expected on Si, relative to PK+ pollen that is in contact with PS that does not have as thick an adsorbed water layer.

One might ask how the complex morphology of the pollen particle may affect its adhesion force. In the AFM adhesion forces measured in this paper, we observed only one spike making contact with the substrate surface. In this case the geometrical characteristics of dry adhesion are governed by the tip radius of the single spine in contact [22], and the pollen geometrical effect on capillary wet adhesion is additionally dependent on the volume of pollenkitt carried on the pollen. The tip radius of each tip is independent of the arrangement of spikes, i.e., the pollen morphology. The pollenkitt volume is dependent on the morphology, because some morphologies, for example echinate pollens, allow more pollenkitt to be carried in pores and pockets than other varieties [8]. Increased volume generally leads to larger bridges and increased capillary adhesion, as indicated in Eq. (4). However, in our studies the species was held constant and was not varied, hence the volume of pollenkitt per particle will not vary due to morphology. On the contrary, as discussed above, we find that the volume of pollenkitt in the capillary bridge, determined by fitting Eq. (4) to pull-off data, tends to vary according to the pollenkitt wettability on the substrate.

The curved surfaces of pollen might influence the condensation of water on its outer surface as well as on inner pores through the depression of vapor pressure in a highly-curved interface. What we can say is that the capillary adhesion that is being measured involves surfaces covered with pollenkitt already, so that any water condensation would be immediately absorbed into the pollenkitt. We discussed estimates of capillary condensation in pores present on pollens above (presented in detail in supplementary information) and showed that these would result in a negligible volume of water. But, again, we held constant the species and morphology and even if significant it would be a constant in our studies. Without varying the species, and hence sporopollenin structure, it is not possible for us to draw conclusions about morphology effects on water uptake.

The pull-off forces in Fig. 3 are also consistent with the idea that wetting and viscosity properties of pollenkitt lead to marked changes in adhesion behavior of pollen on hydrophobic versus hydrophilic surfaces as a function of humidity. The pull-off adhesion force increases with increasing RH for PK+ pollen on hydrophilic Si, just as observed for PK−. However, the adhesion forces of PK+ are larger than that of PK− interacting with Si at each RH, which is in agreement with the formation of a larger volume capillary neck as more water is taken up at higher humidity, as discussed above (Fig. 4). The RH-dependent behavior of PK+ and PK− follow the expected trends for a wetting fluid on a hydrophilic substrate, and are in agreement with previous measurements with a wide variety of particles [34]. On hydrophobic PS, which might be considered an analog of waxy plant surfaces, the PK− pollen shows essentially no dependence on RH, also in agreement with expectations of water capillary condensation on hydrophobic surfaces [34]. However, a surprising result is observed for PK+ on the hydrophobic PS surface: the adhesion pull-off force first increases with RH, passes through a maximum value at 35% RH, followed by a decrease with increasing RH, as indicated in Fig. 3. This unusual RH-dependent behavior gives entomophilous pollens like sunflower, which carry significant volumes of pollenkitt, the ability to tune adhesion and detachment behaviors in response to changes in humidity. That PK+ pull-off adhesion shows a maximum as a function of RH indicates competing influences on adhesion. As

RH initially increases, the viscosity begins to drop sharply (Fig. 5), which would allow more volume to wet the PS substrate. However, as RH continues to increase, the decrease in viscosity is compensated by an increase in the contact angle of the pollenkitt–water mixture on PS. This leads to a decreased adhesion magnitude due to diminished wetting (smaller θ) value.

4. Conclusion

Pollenkitt-mediated adhesion of sunflower pollen to hydrophilic and hydrophobic surfaces was measured as a function of humidity. The results quantify for the first time the significant water absorption of pollenkitt and the resulting complex dependence of adhesion on humidity. The comparison of pollens with and without pollenkitt indicates that presence of pollenkitt leads to significantly more water uptake compared to cleaned pollens. On hydrophilic Si, adhesion increased with increasing RH for pollens with or without pollenkitt, up to 200 nN at 70% RH. In contrast, on hydrophobic PS, adhesion of pollenkitt-free pollen is independent of RH. Surprisingly, when pollenkitt was present adhesion forces on hydrophobic PS first increased with RH up to a maximum value at 35% RH (~160 nN), and then decreased with further increases in RH. Independent measurement of pollenkitt properties is used with models of capillary adhesion to show that these humidity-dependent changes in pollenkitt wetting and viscosity are responsible for the complex observed adhesion behavior. These findings suggest that on a hydrophilic substrate, water uptake into the pollenkitt as RH increases always leads to increased adhesion force magnitude. However, on a hydrophobic surface, the capillary adhesion is at first increased as water is added to pollenkitt with increasing RH, likely due to a drop in viscosity leading to an increase in volume that wets the substrate during the contact time. However, at higher RH values, the water-laden pollenkitt seems to wet the hydrophobic surface more poorly, leading to diminished adhesion. These observations support a developing understanding of the roles of pollen adhesion in plant reproduction, in pollinator health and ecology, and in human allergy and asthma. In addition, lessons learned from this natural system can provide important bio-inspired designs for novel adhesive systems.

Author contributions

The manuscript was written through contributions of all authors. All authors have given approval to the final version of the manuscript.

Acknowledgments

Acknowledgment is made to AFOSR Grant number FA955010-1-0555 and to NSF Grant number CMMI1130739 for financial support. The authors also thank Professor Victor Breedveld for the using of the rheological instrument to measure the viscosity of pollenkitt.

Appendix A. Supplementary material

The supporting information available on-line provides a diagram of the SDOF approximation, raw AFM frequency shift data, sample calculations supporting the state of water on PK− pollen, optical microscopy of pollenkitt emulsion, plots of PK− and PK+ force-versus-distance curves typical for PS surfaces, and plots showing the predicted dependence of capillary force on filling angle and volume of pollenkitt fluid. Supplementary data associated with this article can be found, in the online version, at http://dx.doi.org/10.1016/j.jcis.2014.11.065.

References

[1] P. Heizmann, D.T. Luu, C. Dumas, Ann. Bot. 85 (2000) 23–27.
[2] J. Ollerton, W.S. Armbruster, D.P. Vazquez, in: N.M. Waser, J. Ollerton (Eds.), Plant-Pollinator Interactions: From Specialization to Generalization, University of Chicago Press, Chicago, 2006, pp. 19–22.
[3] R.J. Mitchell, R.E. Irwin, R.J. Flanagan, J.D. Karron, Ann. Bot. 103 (9) (2009) 1355–1363.
[4] B.J. Howlett, R.B. Knox, J. Heslop-Harrison, J. Cell Sci. 13 (2) (1973) 603–619.
[5] B.G. Pummer, H. Bauer, J. Bernardi, S. Bleicher, H. Grothe, Atmos. Chem. Phys. 12 (5) (2012) 2541–2550.
[6] C.G. Williams, Am. J. Bot. 100 (6) (2013) 1184–1190.
[7] B. Diethart, S. Sam, M. Weber, Grana 46 (3) (2007) 164–175.
[8] E. Pacini, M. Hesse, Flora 200 (5) (2005) 399–415.
[9] P. Li, C.F. Zeng, L.X. Zhang, N.P. Xu, J. Inorg. Mater. 23 (1) (2008) 49–54.
[10] F. Song, H.L. Su, J.J. Chen, W.J. Moon, W.M. Lau, D. Zhang, J. Mater. Chem. 22 (3) (2012) 1121–1126.
[11] F. Song, H.L. Su, J. Han, W.M. Lau, W.J. Moon, D. Zhang, J. Phys. Chem. C 116 (18) (2012) 10274–10281.
[12] Y. Xia, W.K. Zhang, Z. Xiao, H. Huang, H.J. Zeng, X.R. Chen, F. Chen, Y.P. Gan, X.Y. Tao, J. Mater. Chem. 22 (18) (2012) 9209–9215.
[13] D.S. Rimai, L.H. Sharpe, A.S. Meeting, Advances in Particle Adhesion, Gordon and Breach, 1996.
[14] G.M. Zinkl, B.I. Zwiebel, D.G. Grier, D. Preuss, Development 126 (23) (1999) 5431–5440.
[15] E. Dominguez, J.A. Mercado, M.A. Quesada, A. Heredia, Sex. Plant Reprod. 12 (3) (1999) 171–178.
[16] N. Ivleva, R. Niessner, U. Panne, Anal. Bioanal. Chem. 381 (1) (2005) 261–267.
[17] H. Kano, H.O. Hamaguchi, Chem. Lett. 35 (10) (2006) 1124–1125.
[18] R.J. Scott, Mol. Cell. Aspects Plant Reprod. 55 (1994) 49–81.
[19] J. Brooks, G. Shaw, Nature 219 (5153) (1968) 532–533.
[20] J. Brooks, G. Shaw, Chem. Geol. 10 (1) (1972) 69. 69-&.
[21] F.R. Knoll, Zeit Schr Bot. [Festschr Oltmanns] 23 (1930) 609–675.
[22] H. Lin, I. Gomez, J.C. Meredith, Langmuir 29 (9) (2013) 3012–3023.
[23] J.C. Meredith, A. Karim, E.J. Amis, Macromolecules 33 (16) (2000) 5760–5762.
[24] S. Schulz, C. Arsene, M. Tauber, J.N. McNeil, Phytochemistry 54 (3) (2000) 325–336.
[25] E. Pacini, Can. J. Bot.-Rev. Canadienne De Botanique 75 (9) (1997) 1448–1459.
[26] H.E.M. Dobson, Am. J. Bot. 75 (2) (1988) 170–182.
[27] B.J.R. Thio, J.-H. Lee, J.C. Meredith, Environ. Sci. Technol. 43 (12) (2009) 4308–4313.
[28] N.A. Burnham, X. Chen, C.S. Hodges, G.A. Matei, E.J. Thoreson, C.J. Roberts, M.C. Davies, S.J.B. Tendler, Nanotechnology 14 (1) (2003) 1–6.
[29] J.L. Hutter, J. Bechhoefer, Rev. Sci. Instrum. 64 (1993) 1868–1873.
[30] L. Zitzler, S. Herminghaus, F. Mugele, Phys. Rev. B 66 (15) (2002) 155436.
[31] S. Boskovic, J.W.M. Chon, P. Mulvaney, J.E. Sader, J. Rheol. 46 (4) (2002) 891–899.
[32] P. Piffanelli, J.H.E. Ross, D.J. Murphy, Sex. Plant Reprod. 11 (2) (1998) 65–80.
[33] T. Shigetomi, H. Tsuzumi, K. Toi, T. Ito, J. Appl. Polym. Sci. 76 (1) (2000) 67–74.
[34] M. He, A.S. Blum, D.E. Aston, C. Buenviaje, R.M. Overney, R. Luginbuhl, J. Chem. Phys. 114 (2001) 1355.
[35] J. Ally, E. Vittorias, A. Amirfazli, M. Kappl, E. Bonaccurso, C.E. McNamee, H.J. Butt, Langmuir 26 (14) (2010) 11797–11803.
[36] O. Pitois, P. Moucheront, X. Chateau, J. Colloid Interface Sci. 231 (1) (2000) 26–31.
[37] H.J. Butt, M. Kappl, Adv. Colloid Interface Sci. 146 (1–2) (2009) 48–60.
[38] S. Guriyanova, B. Semin, T.S. Rodrigues, H.J. Butt, E. Bonaccurso, Microfluid. Nanofluid. 8 (5) (2010) 653–663.
[39] M.J. Matthewson, Philos. Mag. A – Phys. Condens. Matter Struct. Defects Mech. Prop. 57 (2) (1988) 207–216.
[40] X. Xiao, L. Qian, Lanmguir 16 (2000) 8153.